



Studies of Low and Intermediate Temperature Oxidation of Propane up to 100 Atm in a Supercritical-Pressure Jet-Stirred Reactor

Hao Zhao*, Chao Yan*, Guohui Song, Ziyu Wang, Yiguang Ju

Department of Mechanical and Aerospace Engineering, Princeton University, Princeton, NJ 08544-5263, USA

Received 5 January 2022; accepted 11 July 2022

Available online 7 September 2022

Abstract

The low and intermediate temperature oxidation of propane has been investigated by using a novel supercritical pressure jet stirred reactor (SP-JSR) with and without 20% CO₂ additions at fuel lean and rich conditions at 10 and 100 atm and 500–1000 K. The mole fractions of C₃H₈, O₂, CO, CO₂, CH₂O, C₂H₄, CH₃CHO, and C₃H₆ were quantified by using a micro-gas chromatograph (μ -GC). The experiment showed that different from that of 10 atm, at 100 atm only a weak negative temperature coefficient (NTC) behavior was observed because of the significant shift of the intermediate temperature HO₂ chemistry to lower temperature. In addition, at 100 atm, existing models in literatures could successfully capture the onset temperatures of the low and intermediate chemistry, while under-predict the fuel oxidation quantitatively and fail to capture the NTC behavior between 650 and 780 K at both fuel lean and rich conditions. Similar discrepancy was observed in studies of n-butane and dimethyl ether (DME) oxidations in literatures, implying that there existed large uncertainties in hierarchy model development of fuels with low temperature chemistries at extremely high pressures. Reaction pathways and sensitivity analyses showed that RO₂ competing reactions through (P1) RO₂ = QOOH, (P2) RO₂ = C₃H₆ + HO₂, (P3) RO₂ + CH₂O/HO₂ = RO₂H + HCO / O₂ dominated the low and intermediate temperature chemistries, followed by HO₂ / H₂O₂ chemistry at 100 atm, which differed from the dominant pathway through QOOH consumption reactions at lower pressures. Especially, P3 is a new pathway of RO₂ consumption at high pressures, which was not observed in importance at low pressures. Special attention should be paid to the accurate computations of n-C₃H₇O₂ / i-C₃H₇O₂ + CH₂O and n-C₃H₇O₂ / i-C₃H₇O₂ + in the P3 pathway and n-C₃H₇O₂ / i-C₃H₇O₂ decomposition reactions in the P2 pathway at high pressures.

© 2022 The Combustion Institute. Published by Elsevier Inc. All rights reserved.

Keywords: Supercritical kinetics; Propane; Jet-stirred reactor; Ultra-high pressure; Low temperature chemistry

1. Introduction

Supercritical combustion has been paid increasing attentions to applications in advanced gas turbines and engines due to its higher thermodynamic

* Corresponding authors.

E-mail addresses: cgsq725525@gmail.com (H. Zhao), chaoy@princeton.edu (C. Yan).

efficiency, leaner fuel flammability, and lower emissions at high pressures [1–4]. However, under supercritical conditions (100–300 atm), intermolecular attractions cannot be ignored, while non-ideal fluid behavior may result in significant deviations of reaction kinetics and thermodynamic and transport properties from the ideal-gas consideration. For example, under ultra-high pressures, multiple-body collisions begin to play an important role in rate constant computations from typical isolated binary collisions in most gas-phase kinetic modeling [5,6], and result in unusual pressure dependencies. Collisional cross-section area may depart in the real-fluid potential of interactions. Thermodynamic properties, such as heat capacity, of CO_2 and H_2O can be 50% different from ideal-gas values above 200 atm [7]. Therefore, kinetic experiments and theoretical computations at high pressures above 100 atm are highly needed for investigating the supercritical combustion chemistry in practical high-pressure engine systems.

In theoretical study, Kogekar et al. [8] simulated real-fluid oxidation of n-dodecane / O_2 / N_2 mixtures using Redlich-Kwong (RK) equation of state (EoS) and provided the computation methods of thermodynamic properties and chemical potentials in the simulation. Li et al. [9] incorporated real-fluid behaviors into hydrogen oxidation simulations in supercritical H_2 / H_2O / CO_2 mixtures using Peng-Robinson (PR) EoS. However, empirical methods in [8,9] are lack of physical insights of molecular interactions at high pressures. Bai et al. [7] constructed the supercritical computation code by using the theoretical Virial EoS and real-fluid partition functions and studied the real-fluid impact on properties of substance and molecules. In experiments, unfortunately, only a few research apparatuses, such as shock tube [8,10], high pressure laminar flow reactor [11–14], and supercritical-pressure jet-stirred reactor (SP-JSR) [5,6,15] in the combustion field can be used to study the supercritical reaction chemistry. Typically, the high-pressure laminar flow reactor is difficult to maintain a uniform temperature distribution and requires a long residence time (above 10 s) at high pressures, where the negative temperature coefficient (NTC) behavior is very difficult to be observed [11]. Shock tube has challenges in flow residence time (10–20 ms) of practical engines and is mainly used for high temperature ignition study, while the low temperature fuel chemistry is difficult to cover. Instead, the supercritical-pressure jet-stirred reactor recently developed by Zhao et al. [5] provides a new experimental platform for studying supercritical fuel chemistry and overcomes the challenges above. The SP-JSR covers a wide range of temperatures (295–1200 K) and pressures (10–200 atm) with a well-defined flow residence time (0.1–1.0 s) close to practical engines and a uniform temperature distribution (± 3 K). We recently studied the low and intermediate tem-

perature chemistries of n-butane [5], dimethyl ether (DME) [6] and methanol [15] at 100 atm using the SP-JSR, and observed weak NTC behaviors of n-butane and DME and a novel NTC pathway of methanol.

Propane is the simplest alkane exhibiting the two-stage oxidation behavior. Its kinetic study is very crucial for hierarchy model development of larger alkanes with low temperature chemistries. The study of propane oxidation chemistry has been performed in flow reactor [13,16], JSR [17,18], shock tube [19–21], and rapid compression machine (RCM) [22,23]. Several models, such as AramcoMech 3.0 [24], USC Mech [25], Hashemi Mech [13], Polimi Mech [26], describing the oxidation of propane have been developed based on the experimental data above. However, high-pressure (above 40 bar) experimental data is lacking for the low temperature chemistry of propane, and its supercritical combustion/oxidation kinetics remains unknown. Therefore, in this study, we perform the propane oxidation at 10 atm in the SP-JSR and use the four propane models [13,24–26] above to compare with the experimental measurements made by the SP-JSR. To study the oxidation chemistry of propane at supercritical conditions and extend the available data toward engine conditions, this paper presents the experimental and modeling results of propane oxidation at fuel lean and rich conditions with and without 20% CO_2 additions at 100 atm and 500–1000 K by using SP-JSR. The mole fractions of C_3H_8 , O_2 , CO , CO_2 , CH_2O , C_2H_4 , CH_3CHO , and C_3H_6 are quantified by using a micro-gas chromatograph (μ -GC). Moreover, the effect of supercritical CO_2 on the propane oxidation is also investigated by adding 20% CO_2 to the reactant mixture at 100 atm. Then, the high-pressure, low and high temperature reaction pathways of propane are analyzed with identification of key reactions.

2. Experimental methods and kinetic models

Experiments of the propane oxidation are performed in the SP-JSR system, as is shown in Fig. 1. The SP-JSR is a spherical bulb with an internal volume of 0.5 cm^3 . It owns 4 fingers with 2 jets (0.2 mm I. D.) on each finger at the center of the bulb, which enables optimized spray directions for intense turbulence and homogenous mixing. The quartz reactor is placed inside a stainless-steel pressure-resistant jacket. The inside and outside pressures of the reactor are balanced by the bath gas flow to reach the high-pressure conditions. The gasses issuing from the SP-JSR exit are sampled by a quartz sonic nozzle, and then equilibrate their pressure with vacuum generated by a dry pump. The experimental system is designed for experiments over 10–200 atm and 298–1200 K tempera-

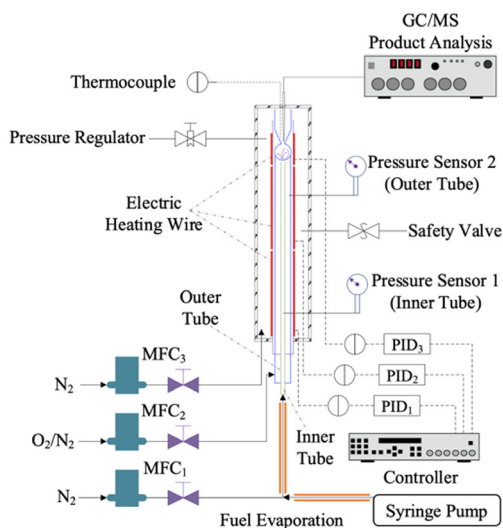


Fig. 1. Schematic of the SP-JSR setup.

ture range. The descriptions of the SP-JSR and its jet and heating arrangements are in details in the literature [5]. Propane is fed to the system through a pressurized gas cylinder. The gas flow rates are controlled by high-pressure mass flow controllers (Brooks, SLA5800) and gas samples are quantified by using GC-TCD (Inficon 3000) within 5% measurement uncertainty [27–29]. The axial temperature profiles under the experimental flow conditions are measured by using reactive mixtures in the present experiments in 1 mm steps along the JSR bulb and are plotted in Fig. S1 of the Supplementary Material, where the temperature variation is within ± 3 K between 500 and 1000 K. The details of the temperature profile measurement are elsewhere in [5].

The experiment is performed at fuel lean and rich conditions with and without CO_2 additions at 10 and 100 atm between 500 and 1000 K, as is shown in Table 1. The residence time of the experiment changes with the temperature to keep a fixed inlet volume flow rate at 0.6 and 6 L/min respectively at 10 and 100 atm at 293 K. Moreover, the residence time is picked with corresponding to the reaction time scale of the oxidation from the computation by using the CHEMKIN software [30].

Table 1
Experimental conditions.

Case	Equivalence ratio	Pressure (atm)	C_3H_8 (%)	O_2 (%)	N_2 (%)	CO_2 (%)	Residence time (s)	Temperature (K)
1	0.20	10	0.324	8.05	91.636	0	0.234–0.13	500–1000
2	0.20	100	0.324	8.05	91.636	0	0.234–0.13	500–1000
3	0.20	100	0.324	8.05	72.383	19.24	0.234–0.13	500–1000
4	1.75	100	0.490	1.40	98.11	0	0.234–0.13	500–1000

Every measurement is repeated two times for the same temperature condition. Four propane models, AramcoMech 3.0 [24], USC Mech [25], Hashemi Mech [13], Polimi Mech [26], are utilized to compare with the experimental measurements made by the SP-JSR. The real gas effect for propane oxidation at 100 atm is small and can be neglected. Figure S2 in the Supplementary Material exhibits the simulation comparison of real-gas and ideal-gas propane oxidations by using Virial EoS [7] at 100 atm. All simulations are performed using the perfect stirred reactor module in the CHEMKIN software [30].

3. Results and discussion

The experimental and modeling results of propane oxidation at 10 atm are plotted in Fig. 2. It is noted that NTC behavior is not observed in the propane oxidation at 10 atm in this experiment due to a relatively short residence time. The model predictions of C_3H_8 , CO , CO_2 , CH_2O , and C_2H_4 by using Aramco Mech and Polimi Mech agree with experimental data reasonably well, while Hashemi Mech and USC Mech exhibit larger discrepancies for predicting most species. Especially, USC Mech is commonly used for high temperature chemistry predictions while is less effective for low and intermediate temperature kinetic study. Moreover, there exists significant errors in predicting the CH_2O mole fraction in these 4 models, implying non-negligible uncertainties in low and intermediate temperature chemistries of propane in existing models. The validation of the fuel evolution against temperature in Fig. 2(a) by using Aramco Mech, Polimi Mech, and Hashemi Mech indicates that the SP-JSR in this study can successfully capture the low-pressure oxidation characteristics against literature models.

Fig. 3 depicts the propane evolution against temperature with and without 20% CO_2 additions at fuel lean conditions (a) and at fuel rich conditions (b), respectively, at 100 atm. Experimental data in Fig 3(a) and (b) shows a clear low temperature chemistry of propane oxidation from 625 K with and without CO_2 additions at both fuel lean and rich conditions at 100 atm. It also exhibits a typical window of NTC behavior from 700 to 780 K. Moreover, it is seen that supercritical CO_2

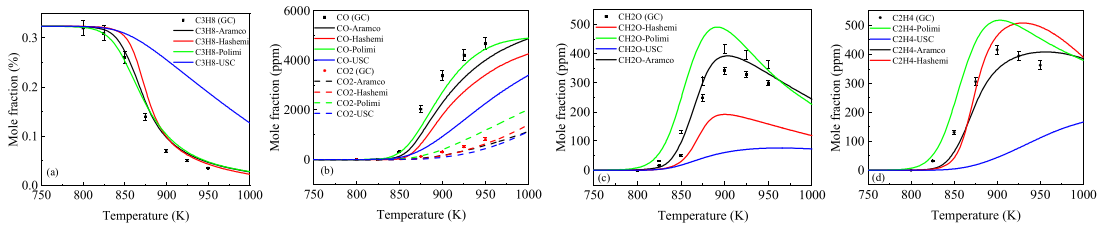


Fig. 2. Mole fractions of C_3H_8 , CO, CO_2 , CH_2O , and C_2H_4 in the oxidation of propane (case 1) at 10 atm.

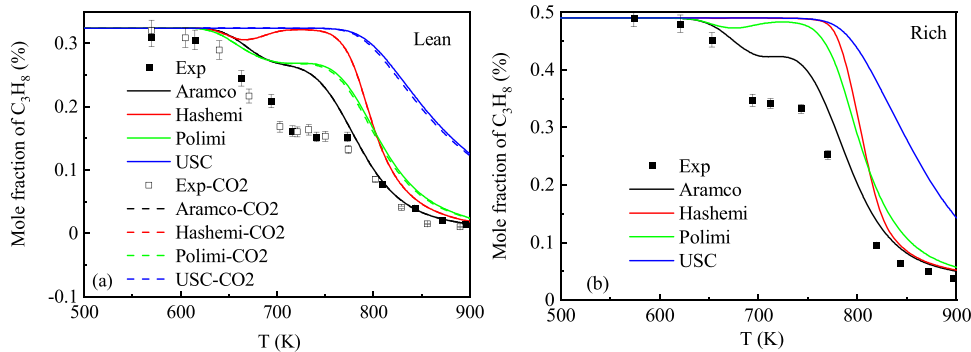


Fig. 3. Temperature evolutions of C_3H_8 in the propane oxidation without CO_2 at fuel lean conditions (case 2), with 20% CO_2 at fuel lean conditions (case 3), and without CO_2 at fuel rich conditions (case 4) at 100 atm.

has limited effect on the low temperature oxidation of propane at 100 atm. As is seen in Fig. 2, the low temperature chemistry is not observed at 10 atm in experiment, while it is dramatically enhanced between 700 and 800 K at 100 atm with a fixed residence time. The intermediate temperature oxidation is shifted from 825 K at 10 atm to around 775 K at 100 atm. It indicates that both the low and intermediate temperature oxidations are accelerated with increasing pressures. We think it is probably due to the enhancement of the third-body collisional reactions, such as 1st and 2nd O_2 addition reactions of the low temperature chemistry at higher pressures.

In comparing the model predictions with experimental data at 100 atm, USC Mech fails to predict the low temperature oxidation of propane at both lean and rich conditions and is not considered as a validation model in the discussion. Aramco Mech, Polimi Mech, and Hashemi Mech successfully capture the onset temperatures of the low and intermediate chemistry, while under-predict the oxidation and fail to capture the NTC behavior between 650 and 780 K at both fuel lean and rich conditions. The NTC behavior is even negligibly observed in Hashemi Mech. Such a large uncertainty in the NTC behavior corresponds with our discussion on the poor predictability of CH_2O mole fraction in Fig. 2(c). Overall, all these models under-predict the oxidation at the NTC region. Similar under-predictions of fuel reactivities have

also been observed in our previous study of n-butane [5] and DME [6] oxidations at 100 atm and lower pressures. The under-predictions of the low-temperature oxidation of DME, n-butane, and propane imply that there exist large discrepancies in a series of pressure-dependent reactions in their low-temperature chemistries, especially at the NTC region at high pressures, such as 1st, 2nd, and 3rd O_2 addition reactions. Therefore, the theoretical computation such pressure-dependent reactions at high pressures with including non-ideal collisions and potentials by using non-Boltzmann transition state theory may need to be highly emphasized for further investigations. Overall, Aramco Mech exhibits the best prediction performance against the experimental data at 10 atm and 100 atm in this study.

To explain the impact of pressure on the propane oxidation and the discrepancy in predicting the NTC behavior, pathway analyses of propane are performed at the fuel lean condition at 10 atm and 880 K (a), the fuel lean condition at 100 atm and 720 K (b), and the fuel rich condition at 100 atm and 720 K (c) by using Aramco Mech, respectively. The schematic of reaction pathways with 20% CO_2 additions (case 3) is similar to Fig. 4 (b) and is not plotted here. If one follows the predictions by the model, the result at 10 atm in Fig. 4 (a) shows that two important fuel radicals, n- C_3H_7 and i- C_3H_7 , are formed from H abstraction reactions of propane by OH and HO_2 radicals, and further

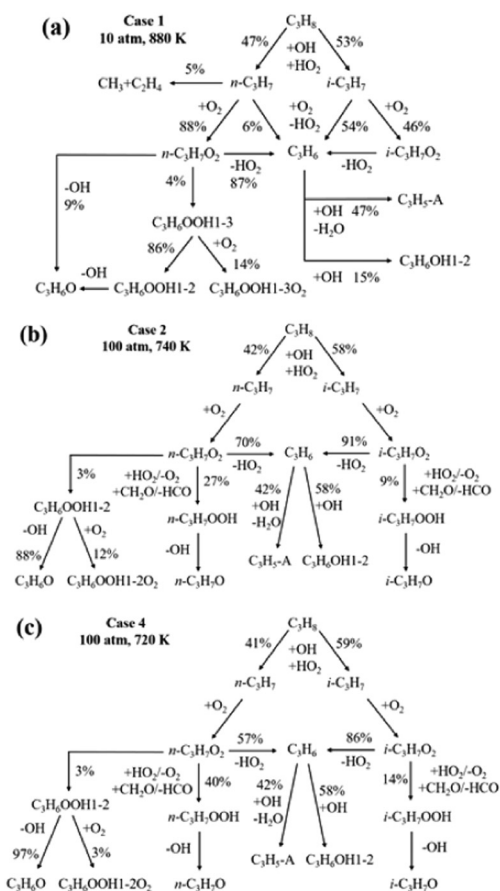


Fig. 4. Reaction pathways for propane at the fuel lean condition at 10 atm and 880 K (case 1) (a), the fuel lean rich condition at 100 atm and 720 K (case 2) (b), and the fuel rich condition at 100 atm and 720 K (case 4) (c) by using Aramco Mech.

form RO_2 ($n\text{-C}_3\text{H}_7\text{O}_2$ and $i\text{-C}_3\text{H}_7\text{O}_2$) through the 1st O_2 addition reaction or produce C_3H_6 through another H abstraction reaction. Then, most RO_2 decomposes to C_3H_6 (above 87%) instead of forming QOOH ($\text{C}_3\text{H}_6\text{OOH}$) through isomerization reactions at low pressures in case 1. Overall, more than 90% of C_3H_8 forms C_3H_6 and then CO and CO_2 through the high temperature chemistry, while the low temperature pathway through QOOH competing reactions is insignificant in Fig. 4 (a), which explains the non-observation of the low temperature chemistry in experiment at 10 atm in case 1.

At 100 atm in Fig. 4 (b) and (c), $n\text{-C}_3\text{H}_7$ and $i\text{-C}_3\text{H}_7$ are also formed from propane in the model simulations. However, different from the pathway at 10 atm in Fig. 4 (a), all these two fuel radicals further form RO_2 through O_2 addition reactions instead of producing C_3H_6 through H abstraction reactions. That is due to the collisional enhance-

ment for pressure-dependent reactions at higher pressures. Then, there are three competing pathways for RO_2 consumptions: (P1) $\text{RO}_2 = \text{QOOH}$, (P2) $\text{RO}_2 = \text{C}_3\text{H}_6 + \text{HO}_2$, (P3) $\text{RO}_2 + \text{CH}_2\text{O} / \text{HO}_2 = \text{RO}_2\text{H} + \text{HCO} / \text{O}_2$. P1 is the typical pathway of the low temperature chemistry, followed by QOOH competing reactions. P2 is the typical pathway of the intermediate temperature chemistry, followed by $\text{HO}_2 / \text{H}_2\text{O}_2$ intermediate temperature chemistry. P3 is a new pathway of RO_2 consumption at high pressures, and is not observed in importance at low pressures. At high pressures to 100 atm, the intermediate temperature HO_2 chemistry is shifted to lower temperatures at the NTC region. P2 becomes dominant at lower temperatures. The boundary between low and intermediate temperature chemistries becomes indistinct at high pressures. Similar results have been observed in our previous study on n-butane and DME oxidations [5,6]. Meanwhile, the new reaction pathway P3 appears due to the dramatic increase of HO_2 and CH_2O concentrations at higher pressures and their intense collisions with RO_2 . Both reaction channels above suppress the typical low temperature pathway through P1, which only accounts for less than 3% consumption rate of RO_2 . The NTC behavior of alkane is commonly explained by QOOH competing reactions at low pressures. However, at high pressures, RO_2 competing reactions through P1-P3 are more dominant. It exactly corresponds with the pathway analysis of n-butane in our previous study [5]. We think the large prediction discrepancy of the NTC behavior in the existing models against experiments may be due to the uncertainty of reaction pathways at low pressures.

Furthermore, to investigate the discrepancy between experiments and model simulations in the NTC and the intermediate temperature region at 100 atm, the sensitivity analyses for propane at the fuel lean (case 2) and rich (case 4) conditions at 100 atm and 720 K by using Aramco Mech are plotted in Fig. 5(a) and (b), respectively. The normalized, first-order propane sensitivity coefficient for the i -th reaction, S_i , is defined as $S_i = (A_i / X_{\text{C}_3\text{H}_8}) (\partial X_{\text{C}_3\text{H}_8} / \partial A_i)$, where A_i is the pre-exponential factor for the i -th rate constant and $X_{\text{C}_3\text{H}_8}$ is the propane mole fraction. It is seen in Fig. 5(a) and (b) that the propane oxidation is largely controlled by the H-abstraction from propane by OH ($\text{C}_3\text{H}_8 + \text{OH} = n\text{-C}_3\text{H}_7 + i\text{-C}_3\text{H}_7 + \text{H}_2\text{O}$), RO_2 competing reactions through P1 ($n\text{-C}_3\text{H}_7\text{O}_2 = \text{C}_3\text{H}_6\text{OOH1-3}$, $\text{C}_3\text{H}_6\text{OOH1-3O}_2 = \text{C}_3\text{KET13} + \text{OH}$, $\text{C}_3\text{H}_6\text{OOH1-3O}_2 = \text{HO}_2 + \text{AC}_3\text{H}_5\text{OOH}$), P2 ($n\text{-C}_3\text{H}_7\text{O}_2 = \text{HO}_2 + \text{C}_3\text{H}_6$, $i\text{-C}_3\text{H}_7\text{O}_2 = \text{C}_3\text{H}_6 + \text{HO}_2$, $\text{HO}_2 + \text{HO}_2 = \text{H}_2\text{O}_2 + \text{O}_2$, $\text{H}_2\text{O}_2 + (\text{M}) = 2\text{OH} + \text{M}$), and P3 ($i\text{-C}_3\text{H}_7\text{O}_2 + \text{CH}_2\text{O} = i\text{-C}_3\text{H}_7\text{O}_2\text{H} + \text{HCO}$, $i\text{-C}_3\text{H}_7\text{O}_2 + \text{HO}_2 = i\text{-C}_3\text{H}_7\text{O}_2\text{H} + \text{O}_2$), and the $\text{CH}_2\text{O}/\text{HCO}$ chemistry. The appearance of sensitive reactions in P1-P3 pathways confirms the state-

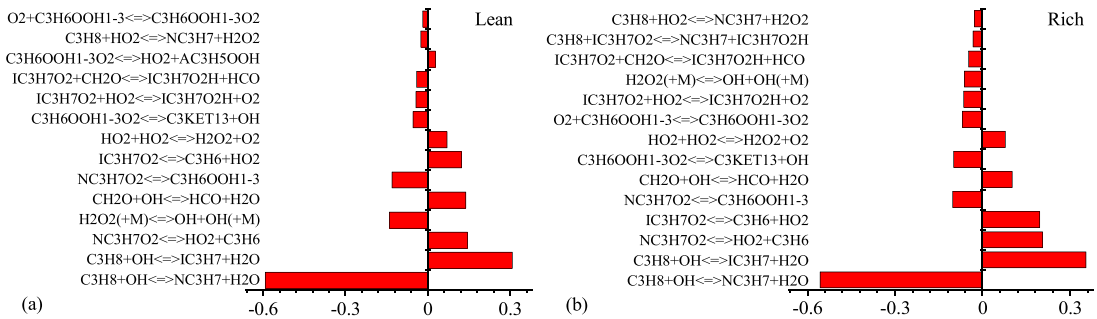


Fig. 5. Sensitivity analyses for propane at the fuel lean (case 2) (a) and rich (case 4) (b) conditions at 100 atm and 720 K by using Aramco Mech.

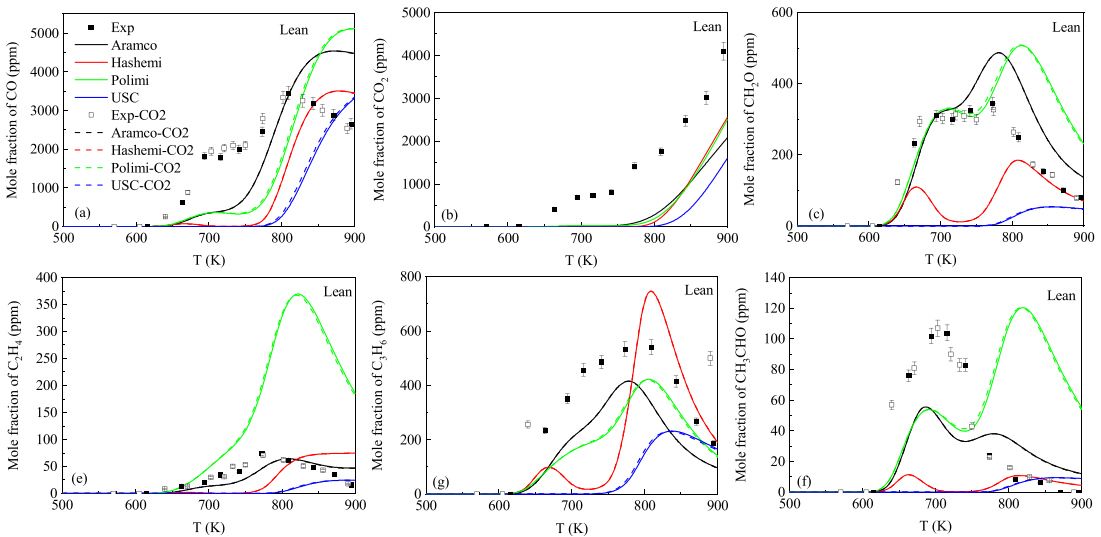


Fig. 6. Temperature evolutions of the mole fraction of CO (a), CO₂ (b), CH₂O (c), C₂H₄ (d), C₃H₆ (e), and CH₃CHO (f) in the propane oxidation without (case 2) and with (case 3) 20% CO₂ additions at the fuel lean condition at 100 atm.

ment of the low temperature oxidation of propane through P1-P3 at 100 atm in the pathway analysis above. Especially, reactions in the H₂O₂/HO₂ chemistry, which are generally important in the intermediate temperature region [31], are also sensitive at 720 K in the NTC region. Therefore, it confirms the statement in the pathway analysis that the intermediate temperature HO₂ chemistry is shifted to lower temperature in the NTC region at 100 atm. Special attention should be paid to the accurate computations of $i\text{-C}_3\text{H}_7\text{O}_2 + \text{CH}_2\text{O} = i\text{-C}_3\text{H}_7\text{O}_2\text{H} + \text{HCO}$ and $i\text{-C}_3\text{H}_7\text{O}_2 + \text{HO}_2 = i\text{-C}_3\text{H}_7\text{O}_2\text{H} + \text{O}_2$ in the P3 pathway and $n\text{-C}_3\text{H}_7\text{O}_2 / i\text{-C}_3\text{H}_7\text{O}_2 = \text{HO}_2 + \text{C}_3\text{H}_6$ in the P2 pathway at high pressures. A further sensitivity analysis of propane at case 1 at 880 K and 10 atm by using Aramco Mech has been plotted in Fig. S3 of the Supplementary Material. It shows that, different from the sensitivity analysis at 100 atm, reactions associated with O₂ additions to QOOH are not sensitive at 10 atm, corresponding with the

weak low temperature reactivity at low pressures. Furthermore, the sensitivity analyses of propane at case 2 at 740 K and 100 atm by using Polimi Mech and Hashemi Mech have been plotted respectively in Fig. S4 and Fig. S5 of the Supplementary Material and are compared with the sensitivity analysis by using Aramco Mech in Fig. 5(a). The sensitivity analysis by using USC Mech is not included as there is no reactivity at the low temperature window in USC Mech. P1-P3 pathways associated with RO₂ consumption are exhibited importance in Aramco Mech, while in Polimi Mech, reactions in P3 are insensitive but O₂ addition reactions to QOOH become very sensitive. In Hashemi Mech, reactions associated with P1, P3, and QOOH consumptions are all insensitive, corresponding with a very weak low temperature reactivity in this model simulation.

The mole fractions of other important products and intermediates, such as CO, CO₂, CH₂O,

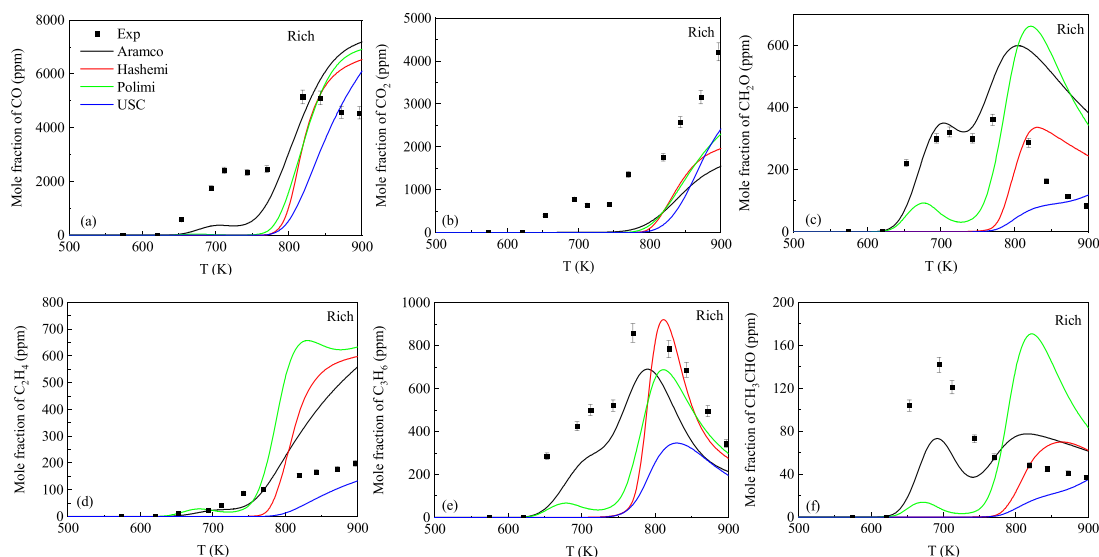


Fig. 7. Temperature evolutions of the mole fraction of CO (a), CO₂ (b), CH₂O (c), C₂H₄ (d), C₃H₆ (e), and CH₃CHO (f) in the propane oxidation without CO₂ additions at the fuel rich condition at 100 atm (case 4).

C₂H₄, C₃H₆, and CH₃CHO at fuel lean and rich conditions are plotted in Fig. 6(a)–(f) and Fig. 7(a)–(f), respectively. At both lean and rich conditions, the low and intermediate temperature oxidation peaks against temperature begin to “merge” to a single peak as the NTC behavior is suppressed due to the shift of the intermediate temperature HO₂ chemistry to lower temperatures at 100 atm. As is seen in Fig. 6, supercritical CO₂ has limited impact on the speciation both in experiment and simulations. Aramco Mech and Polimi Mech generally capture the oxidation characteristics of major products and intermediates in experiments correctly, while over-predict their concentrations in the NTC region significantly, which corresponds with the under-prediction of the propane oxidation at both fuel rich and lean conditions in Fig. 3. Hashemi Mech and USC Mech remain larger discrepancies with experimental data due to missing pathways. For example, the new reaction pathway through P3 does not exist in these two models, making it difficult to capture and analyze the low temperature characteristics of the propane oxidation. It should be noted that the discrepancy between experiment and model simulation for CO and CO₂ productions is still large above 800 K. Therefore, the reactions of CO₂ + H = CO + OH and CO₂ + OH = CO + HO₂ need careful evaluations at supercritical conditions. Such obvious inconsistencies exist in previous n-butane study [5] as well. Overall, Aramco Mech performs the best in these four models, while Polimi Mech exhibits larger uncertainty in predicting C₂H₄ and CH₃CHO mole fractions above 750 K. Kinetic studies of reactions in P2 and P3 relevant to C₂H₄, CH₃CHO, and C₃H₆ may help improve the model perfor-

mance at the NTC and intermediate temperature regions.

4. Conclusion

Supercritical pressure jet stirred reactor provides a valuable platform for performing kinetic studies at low and intermediate temperatures at extreme pressures with a uniform temperature distribution and a short flow residence time. The low and intermediate temperature oxidation of propane has been investigated using SP-JSR with and without 20% CO₂ additions at fuel lean and rich conditions at 10 and 100 atm and 500–1000 K. The mole fractions of C₃H₈, O₂, CO, CO₂, CH₂O, C₂H₄, CH₃CHO, and C₃H₆ are quantified by using a μ -GC. The experiment shows that at 100 atm, a much weaker NTC behavior is observed because the HO₂ intermediate temperature chemistry is substantially shifted to lower temperatures. Supercritical CO₂ has little effect on the low temperature oxidation at 100 atm. Four existing models in literatures are compared to the experimental measurements made by SP-JSR. Aramco Mech, Polimi Mech, and Hashemi Mech successfully capture the onset temperatures of the low and intermediate temperature chemistry, while under-predict the oxidation and fail to capture the NTC behavior between 650 and 780 K at both fuel lean and rich conditions at 100 atm. Similar discrepancy has been observed in our previous study on n-butane and DME oxidation, implying larger uncertainties in hierarchy model development of fuels with low temperature chemistry at extremely high pressures.

Reaction pathways and sensitivity analyses show that RO_2 competing reactions through (P1) $\text{RO}_2 = \text{QOOH}$, (P2) $\text{RO}_2 = \text{C}_3\text{H}_6 + \text{HO}_2$, (P3) $\text{RO}_2 + \text{CH}_2\text{O}/\text{HO}_2 = \text{RO}_2\text{H} + \text{HCO}/\text{O}_2$ dominate the low and intermediate temperature chemistries, followed by $\text{HO}_2/\text{H}_2\text{O}_2$ chemistry, at 100 atm, which differ from the dominant pathway through QOOH consumption reactions at lower pressures. Especially, P3 is a new pathway of RO_2 consumption at high pressures, which is not observed in importance at low pressures. There still exists large uncertainty in predicting major products and intermediates in the NTC region. Special attention should be paid to the accurate computations of $\text{n-C}_3\text{H}_7\text{O}_2/\text{i-C}_3\text{H}_7\text{O}_2 + \text{CH}_2\text{O} = \text{i-C}_3\text{H}_7\text{O}_2\text{H} + \text{HCO}$ and $\text{n-C}_3\text{H}_7\text{O}_2/\text{i-C}_3\text{H}_7\text{O}_2 + \text{HO}_2 = \text{i-C}_3\text{H}_7\text{O}_2\text{H} + \text{O}_2$ in the P3 pathway and $\text{n-C}_3\text{H}_7\text{O}_2/\text{i-C}_3\text{H}_7\text{O}_2 = \text{HO}_2 + \text{C}_3\text{H}_6$ in the P2 pathway at high pressures.

Declaration of Competing Interest

We declare that we have no financial and personal relationships with other people or organizations that can inappropriately influence our work, there is no professional or other personal interest of any nature or kind in any product, service and/or company that could be construed as influencing the position presented in, or the review of, the manuscript entitled.

Acknowledgement

This work was partly supported by ARO grant W911NF-16-1-0076 and the DOE BES award DE-SC0021135.

Supplementary materials

Supplementary material associated with this article can be found, in the online version, at doi:10.1016/j.proci.2022.07.086.

References

- [1] R.D. Reitz, Combustion and ignition chemistry in internal combustion engines, *Int. J. Engine Res.* 14 (2013) 411–415.
- [2] G.P. Sutton, O. Biblarz, *Rocket Propulsion Elements*, John Wiley & Sons, 2016.
- [3] W. Liang, W. Li, C.K. Law, Laminar flame propagation in supercritical hydrogen/air and methane/air mixtures, *Proc. Combust. Inst.* 37 (2019) 1733–1739.
- [4] H. Zhao, N. Zhao, C. Yan, Z. Zhang, Y. Ju, Studies of multi-channel spark ignition characteristics of n-pentane/air mixture under fuel lean conditions in a spherical bomb, *Combust. Flame* 212 (2020) 337–344.
- [5] H. Zhao, C. Yan, T. Zhang, G. Ma, M. Souza, C. Zhou, Y. Ju, Studies of high-pressure n-butane oxidation with CO_2 dilution up to 100bar using a supercritical-pressure jet-stirred reactor, *Proc. Combust. Inst.* 38 (2021) 279–287.
- [6] C. Yan, H. Zhao, Ziyu Wang, et al., Low- and intermediate-temperature oxidation of dimethyl ether up to 100 atm in a supercritical pressure jet-stirred reactor, *Combust. Flame* (2022) In press, doi:10.1016/j.combustflame.2022.112059.
- [7] J. Bai, P. Zhang, C.-W. Zhou, H. Zhao, Theoretical Studies of Real-Fluid Oxidation of Hydrogen Under Supercritical Conditions by Using the Virial Equation of State, *Combust. Flame* (2022) In press, doi:10.1016/j.combustflame.2021.111945.
- [8] G. Kogekar, C. Karakaya, G.J. Liskovich, M.A. Oehlschlaeger, S.C. DeCaluwe, R.J. Kee, Impact of non-ideal behavior on ignition delay and chemical kinetics in high-pressure shock tube reactors, *Combust. Flame* 189 (2018) 1–11.
- [9] G. Li, Y. Lu, P. Glarborg, Development of a detailed kinetic model for hydrogen oxidation in supercritical $\text{H}_2\text{O}/\text{CO}_2$ mixtures, *Energy Fuels* 34 (2020) 15379–15388.
- [10] J. Shao, R. Choudhary, D.F. Davidson, R.K. Hanson, S. Barak, S. Vasu, Ignition delay times of methane and hydrogen highly diluted in carbon dioxide at high pressures up to 300bar, *Proc. Combust. Inst.* 37 (2019) 4555–4562.
- [11] H. Hashemi, J.M. Christensen, S. Gersen, H. Levinsky, S.J. Klippenstein, P. Glarborg, High-pressure oxidation of methane, *Combust. Flame* 172 (2016) 349–364.
- [12] H. Hashemi, J.G. Jacobsen, C.T. Rasmussen, J.M. Christensen, P. Glarborg, S. Gersen, M. van Essen, H.B. Levinsky, S.J. Klippenstein, High-pressure oxidation of ethane, *Combust. Flame* 182 (2017) 150–166.
- [13] H. Hashemi, J.M. Christensen, L.B. Harding, S.J. Klippenstein, P. Glarborg, High-pressure oxidation of propane, *Proc. Combust. Inst.* 37 (2019) 461–468.
- [14] R.X. Fernandes, K. Luther, J. Troe, Falloff curves for the reaction $\text{CH}_3 + \text{O}_2 (+ \text{M}) \rightarrow \text{CH}_3\text{O}_2 (+ \text{M})$ in the pressure range 2–1000 bar and the temperature range 300–700 K, *J. Phys. Chem. A* 110 (2006) 4442–4449.
- [15] Z. Wang, H. Zhao, C. Yan, et al., Methanol oxidation up to 100 atm in a supercritical pressure jet-stirred reactor, *Proc. Combust. Inst.* (2022) Accepted for oral presentation.
- [16] D.N. Koert, D.L. Miller, N.P. Cernansky, Experimental studies of propane oxidation through the negative temperature coefficient region at 10 and 15 atmospheres, *Combust. Flame* 96 (1–2) (1994) 34–49.
- [17] M. Cathonnet, J.C. Boettner, H. James, Experimental study and numerical modeling of high temperature oxidation of propane and n-butane, *Symp. Combust.* 18 (1981) 903–913.
- [18] M. Cord, B. Husson, J.C. Lizardo Huerta, et al., Study of the Low Temperature Oxidation of Propane, *J. Phys. Chem. A* 116 (2012) 12214–12228.
- [19] O. Penyazkov, K. Ragothar, A. Dean, B. Varatharajan, Autoignition of propane–air mixtures behind reflected shock waves, *Proc. Combust. Inst.* 30 (2005) 1941–1947.

- [20] K.-Y. Lam, Z. Hong, D. Davidson, R. Hanson, Shock tube ignition delay time measurements in propane/O₂/argon mixtures at near-constant-volume conditions, *Proc. Combust. Inst.* 33 (1) (2011) 251–258.
- [21] G. Agafonov, A. Tereza, Autoignition of propane behind shock waves, *Russ. J. Phys. Chem. B* 9 (2015) 92–103.
- [22] S.M. Gallagher, H.J. Curran, W.K. Metcalfe, D. Healy, J.M. Simmie, G. Bourque, A rapid compression machine study of the oxidation of propane in the negative temperature coefficient regime, *Combust. Flame* 153 (1–2) (2008) 316–333.
- [23] E.E. Dames, A.S. Rosen, B.W. Weber, C.W. Gao, C.-J. Sung, W.H. Green, A detailed combined experimental and theoretical study on dimethyl ether/propane blended oxidation, *Combust. Flame* 168 (2016) 310–330.
- [24] C.-W. Zhou, Y. Li, U. Burke, C. Banyon, K.P. Somers, et al., An experimental and chemical kinetic modeling study of 1, 3-butadiene combustion: ignition delay time and laminar flame speed measurements, *Combust. Flame* 197 (2018) 423–438.
- [25] H. Wang, X. You, A.V. Joshi, S.G. Davis, A. Laskin, F. Egolfopoulos, et al. USC 2.0 Mech (2007) http://ignis.usc.edu/USC_Mech_II.htm/.
- [26] E. Ranzi, C. Cavallotti, A. Cuoci, A. Frassoldati, M. Pelucchi, T. Faravelli, New reaction classes in the kinetic modeling of low temperature oxidation of n-alkanes, *Combust. Flame* 162 (2015) 1679–1691.
- [27] H. Zhao, A.G. Dana, Z. Zhang, et al., Experimental and modeling study of the mutual oxidation of N-pentane and nitrogen dioxide at low and high temperatures in a jet stirred reactor, *Energy* 165 (2018) 727–738.
- [28] H. Zhao, L. Wu, C. Patrick, Z. Zhang, Y. Rezgui, X. Yang, G. Wysocki, Y. Ju, Studies of low temperature oxidation of n-pentane with nitric oxide addition in a jet stirred reactor, *Combust. Flame* 197 (2018) 78–87.
- [29] H. Zhao, J. Fu, F.M. Haas, Y. Ju, Effect of prompt dissociation of formyl radical on 1, 3, 5-trioxane and CH₂O laminar flame speeds with CO₂ dilution at elevated pressure, *Combust. Flame* 183 (2017) 253–260.
- [30] <<http://www.reactiondesign.com/products/chemkin/chemkin-pro/>>
- [31] H. Zhao, Z. Zhang, Y. Rezgui, N. Zhao, Y. Ju, Studies of high pressure 1, 3-butadiene flame speeds and high temperature kinetics using hydrogen and oxygen sensitization, *Combust. Flame* 200 (2019) 135–141.